Studying Laser Damage Limits in High-Power Lasers and Accelerator Equipment

Tahsinur Rahman[1], Viviana Vladutescu[1], Mikhail Polyanskiy[2], William Li[2], Dismas Choge[2], Marcus Babzien[2], Vikas Teotia[2], Mark Palmer[2], Tianyi Zhao[1], Joseph Rukaj[1], Jorge Chavez[1], Mithila Islam[1], Oscar Situ[1], Brandon Palencia[1], Li Geng[1], Lufeng Leng[1], Giovanni Ossala[1]
[1]CUNY New York City College of Technology, Brooklyn, NY, 11201, USA; [2]Brookhaven National Laboratory, Upton, NY, 11973, USA

Abstract

In this study, we present the design, fabrication, and application of a custom magnetic system developed to support high-field laser-electron interaction experiments at the Accelerator Facilities Division (AFD) of Brookhaven National Laboratory (BNL). The magnet was designed using electromagnetic simulation platforms, include Simulia OPERA and Rat-GUI to achieve the required field strength and spatial profile for precise manipulation and energy characterization of relativistic electron bunches. Following optimization, the final coil winding geometry was implemented by the Superconducting Magnet Division (SMD), where the completed magnet underwent performance validation. The magnet was integrated into the Ultrafast Electron Diffraction (UED) beamline at AFD where it served as a magnetic spectrometer to intercept the electron beam and resolve the energy distribution of the electron bunches. This energy characterization is important in preparing the electron beam for interaction with the Ultrafast High-Power (UFHP) laser system. By enabling fine energy resolution of the bunches, the magnet allows for synchronization of the electron-laser interaction conditions. Building on this setup, we performed a Laser-Induced Damage Threshold experiment of Beta-Barium Borate (BBO) crystals, used eventually in the Optical Parametric Amplifier (OPA) stages of a Long Wave-Infrared (LWIR) UFHP laser system. The 800nm Near-Infrared (NIR) Ti:Sapphire laser outputs of the UFHP system to probe the nonlinear optical response and damage thresholds of BBO crystal and other optical materials. Post-experiment analysis using optical and electron microscopy revealed detailed damage structure, providing insights into the material behavior under high-intensity laser exposure. As part of this work, we utilized MATLAB and 3DOptix to analyze the experimental results, including beam profile analysis and damage threshold quantification and contributed to building and aligning the optical system. This projected helped me understanding of accelerator systems, from magnetic design to electron beam manipulation to laser-electron interactions and diffraction. Working at BNL, I gained hands-on experience with high-level physics and tools like OPERA, Rat-GUI, MATLAB, General Particle Tracer (GPT) and 3DOptix, contributing to both experimental setup and analysis. These skills enhanced my research experience and offered me a different view on the life of a scientist and engineer.

Introduction

Particle accelerators are important systems in modern science and technology, allowing controlled manipulation of charged particle beams for applications ranging from fundamental physics research, medical diagnostics and therapy, materials science, industrial processing and many more [1]. In these systems, charged particles like electrons or protons are accelerated to very high energy from the electric and magnetic field.

- Electric fields are generated by the RF cavities, which accelerate charged particles by doing work on them along their velocity direction.
- Magnetic fields, produced by dipoles, quadrupoles, and solenoids which steer and focus the beam, changing its direction without changing their kinetic energy.
- Laser systems generate electrons beams via photocathode illumination, supporting advanced beam diagnostics and plasma-based acceleration techniques.

The UED facility at BNL AFD shown in Fig. 1 we utilized a high-intensity 3 MeV electron beam to characterize the performance of the system. The electron beams were generated by the photocathode RF gun driven by a UV pulse, the third harmonic, of a Ti:Sapphire laser [2]. This setup allowed us to measure the electron diffraction with temporal resolution as fine as 200 fs. The laser system was synchronized to the RF source, which delivered near-infrared pump pulses for initiating ultrafast dynamics in samples.

In addition to these experiments, we perform Laser-Induced Damage Threshold (LIDT) experiments using the Ti:Sapphire NIR (800nm) laser on different optical samples. These samples include Fused Silica (SiO_2), BBO crystal (BaB_2O_4), Titanium-doped Sapphire crystal, and KRS-5. This laser has a pulse duration of <100 fs with repetition rate of 240 Hz. We vary the energy (in ranges of μJ) and number of shots applied to the sample to determine the damage threshold.

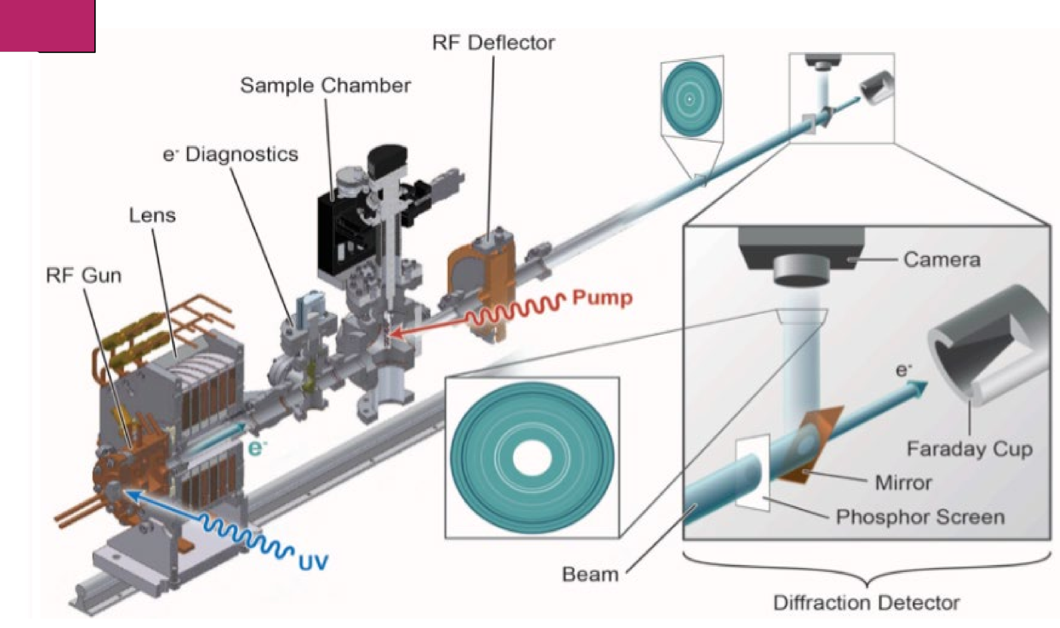

Fig. 1: Linear Accelerator at AFD UED facility [3].

Results

1. Superconducting Magnets

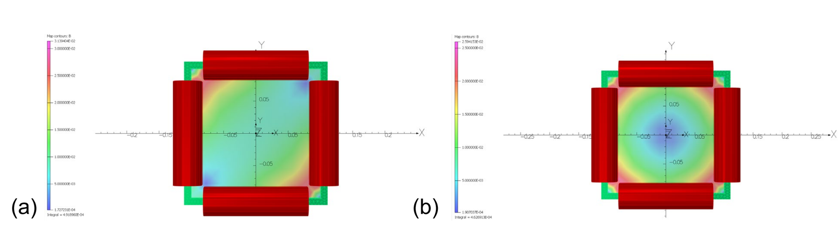

Fig. 2: (a) Dipole and (b) Quadrupole magnetic field mapping simulation on OPERA.

In Simulia Opera, we simulated the dipole and quadrupole magnets to understand their magnetic properties using different B-H materials to perform nonlinear magnetostatic analysis as seen in Fig. 2(a)-(b).

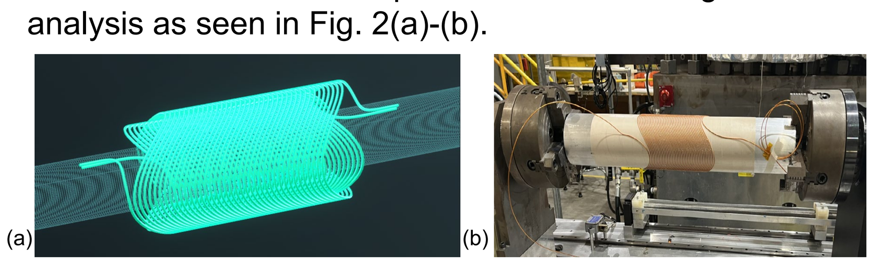

Fig. 3: (a) Rat-GUI Simulation and (b) Physical Winding of the CCT quadrupole magnet design using Nb-Ti wire.

In Rat-GUI, we designed a Canted Cosine Theta (CCT) quadrupole magnet as seen in Fig. 3(a) We exported the files and using MATLAB, we averaged 4-coordinates for each coils making it easier for the engineers to process the data.

Fig. 5: Picture of me holding the magnet.

Using the Direct Winding Machine at SMD, the Niobium-Titanium (Nb-Ti) wires were winded on the fiber glass platform on the aluminum tube as seen in Fig. 3(b). After the wiring process complete, the platform was coated with Blue Epoxy as seen in Fig. 5.

2. Electron Beam

We simulated the beam distribution on GPT software to understand the importance of emittance, space-charge effects and solenoid current adjustments to focus at a specific position along the transverse axis.

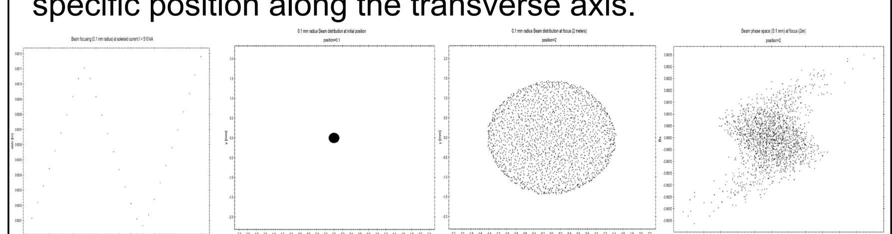

Fig. 6: Beam focusing at 2 meter position with 510 kA solenoid current. **Fig. 7:** Initial beam distribution at position 0.1m. **Fig. 8:** Beam distribution at focused position (2m). **Fig. 9:** Phase space of the beam at focused position.

The solenoid current was set to 510 kA to focus the beam at a 2-meter position, as shown in Fig. 6. Initially, the beam with a 0.1 mm radius appears tightly confined (Fig. 7), but expands significantly by the focal plane due to space charge forces (Fig. 8). These mutual Coulomb repulsions among electrons lead to emittance growth and noticeable distortion in the beam's phase space, as shown in Fig. 9.

Fig. 11: Solenoid Lenses at UED facility.

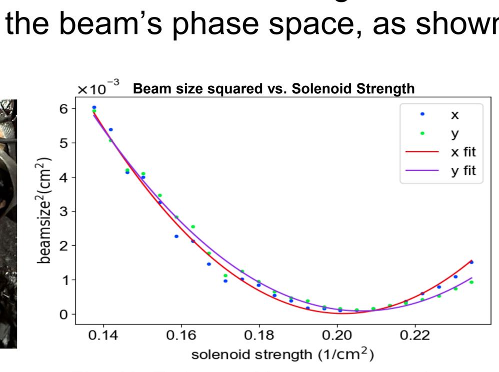

Fig. 12: Emittance Measurements using Solenoid Scan.

The current of solenoid lenses (shown in red in Fig. 11) was adjusted to perform this emittance measurements. We can see squared beam size decrease with increasing solenoid strength, reaching a minimum beam size at the focus in Fig. 12. The parabolic fit help determine the waist position for emittance analysis.

3. Laser and Optics

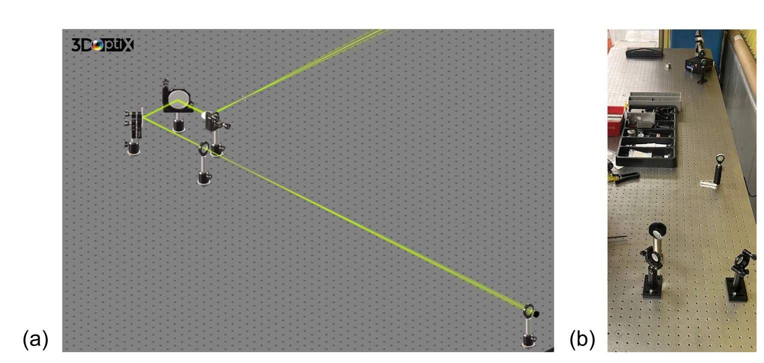

Fig. 13: a) 3DOptix Simulation and b) Physical Experimental Setup

The 3DOptix simulation (Fig. 13a) replicates the experimental setup (Fig. 13b) used to study beam collimation. The parabolic mirror redirects and focuses the beam precisely along the desired path with minimal divergence, highlighting the importance of precise alignment.

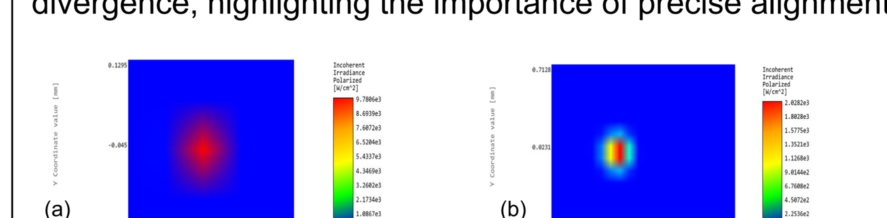

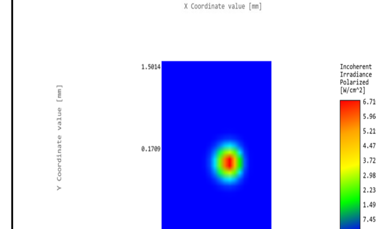

Fig. 14: 3DOptix simulation of collimated beam with (a) ideal alignment, (b) 1° tilt, and (c) 2° tilt of the parabolic mirror.

These three irradiance maps show the effect of tilting a parabolic mirror by 1 degree on beam collimation. Initially, the beam is tightly focused with high peak intensity as shown in Fig. 14(a) After tilting the mirror, the becomes elongated and less collimates shown in Fig. 14(b). The intensity is further reduced and spatially dispersed in the final frame in Fig. 14(c).

4. Laser Induced Damage Threshold

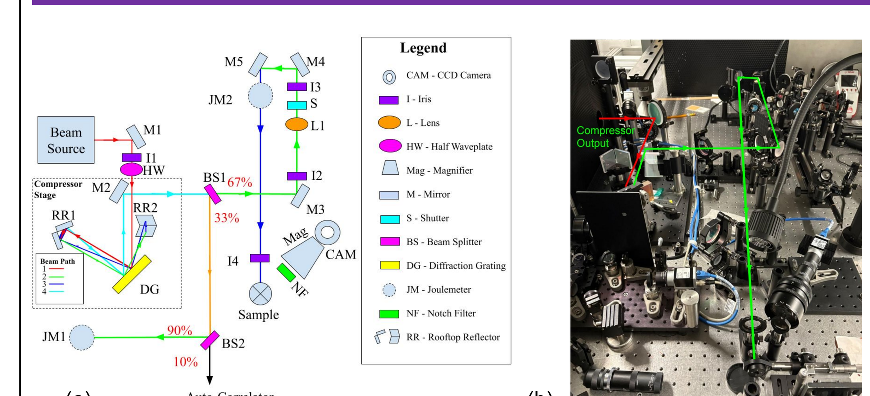

Fig. 15: (a) Visualization and (b) Physical Setup of the LIDT experiment.

In this experiment, we retrieved and analyzed the beam profile using MATLAB to determine the beam radius shown in Fig. 15. For the fused silica wedge (FSW) sample, we determined the damage threshold at 736 ± 8 μJ with calculated fluence of 1.866 J/cm^2 with 2400 shots. On the other hand, we looked into the damage spot on the sample under the laser microscopy at Instrumentation Division, seen in Fig. 16.

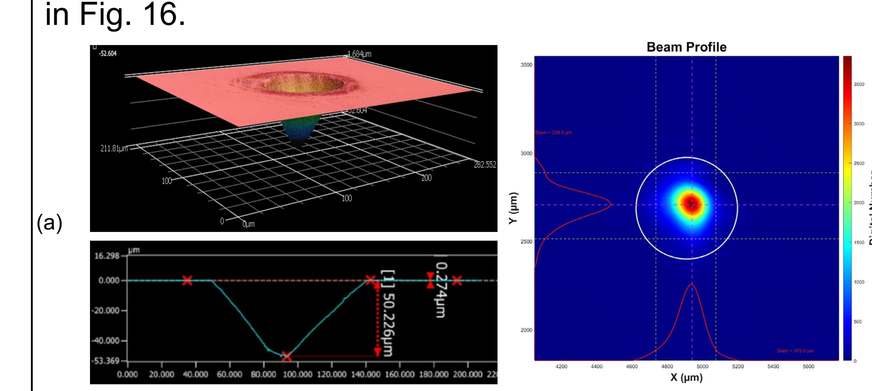

Fig. 15: Beam profile retrieved from the CCD camera.

Fig. 16(a)-(c): Damaged spot analysis of the Fused Silica Sample under Keyence Laser Microscope.

Conclusion and Future Work

Through this project, we gained a comprehensive understanding of how a particle accelerator operates, from magnetic field generation and beam steering to electron dynamics and laser-based diagnostics. Using tools like OPERA and Rat-GUI, we learned how magnetic fields are precisely engineered to manipulate and analyze relativistic electron beams. We explored the electromagnetic foundations of accelerator magnets and translated simulations to real-world hardware via precision winding techniques.

We then studied electron beam propagation using GPT simulations, examining how solenoid fields, space-charge effects, and beam emittance shape the transport and focus of high-energy beams. This gave us insight into delicate balance of forces that control charged particle motion in accelerator environments. To bridge the connection between electron and laser systems, we modeled and constructed an optical beamline in 3DOptix and validated it experimentally, highlighting the importance of precise alignment and optical design for the laser-electron interaction experiments. Finally, we conducted a LIDT experiment, using the femtosecond focused laser pulses to probe the response of different optical materials. Future work includes LIDT of optical samples such as Cadmium Telluride (CdTe), Zinc Selenide (ZnSe), Thallium Bromoiodide (KRS-5) using a 5TW 2ps CO_2 laser (9.2 μm).

References

[1] E. J. N. Wilson, *An Introduction to Particle Accelerators*, Oxford University Press (2001).

[2] Brookhaven National Laboratory, *UED – Brookhaven Ultrafast Electron Diffraction*, beamNetUS, from https://www.beamnetus.org/ued.

[3] P. Zhu, et. al, *Femtosecond Time-resolved MeV Electron Diffraction*, (2015), New J. Phys. 17 063004. https://doi.org/10.48550/arXiv.1304.5176.

Acknowledgements

This work was supported in part by the U.S. Department of Energy, Office of Science, Office of Workforce Development for Teachers and Scientists (WDTS) under the Visiting Faculty Program (VFP). Additionally, I would like to acknowledge the invaluable guidance and support of Jason Becker, John Escallier, Christopher Tamargo, Michael Hartsough, Michael Anerella, and ND from the Superconducting Magnet Division and Jhair Alzamora, Paul Jacob, Karl Kusche, and Anusorn Lueangaramwong from the Accelerator Facilities Division at Brookhaven National Laboratory. Their collective expertise and encouragement were essential to every stage of this work—from early design discussions and simulation troubleshooting to prototype fabrication and testing.

U.S. DEPARTMENT of ENERGY

www.bnl.gov

Brookhaven National Laboratory